A REVIEW OF SOME DEVELOPMENTS IN RAY TRACING AT THE NAVAL AIR DEVELOPMENT CENTER

by

C.L. Bartberger
Naval Air Development Center
Johnsville, Pa., U.S.

INTRODUCTION

The Naval Air Development Center has a comprehensive ray-tracing program which has been extensively used for a number of years not only by our own laboratory, but also by other naval activities and private contractors. In this paper I shall present a brief overall description of the program and shall then describe in somewhat more detail the so-called Target Ray Routine, which searches for and computes the various rays which propagate from a specified source location to a specified receiver location, and combines the rays to compute an effective resultant propagation loss. This will be followed by a few comparisons of ray theory with normal mode theory and with experimental data. The paper will conclude with a few remarks about a suggested technique for ray computation based on a more general type of velocity profile than is currently being used.

GENERAL DESCRIPTION

The NAVAIRDEVCEN ray-tracing program [Ref. 1] is based on a horizontally stratified ocean model consisting of a flat horizontal bottom and a single velocity profile. The velocity profile may be read into the program either as a table of sound speed versus depth

or temperature and salinity versus depth. In the latter case, the sound speed is computed from Wilson's equations [Ref. 2]. The data may be expressed in either English or metric units. Two options are available for curve-fitting, either straight lines or curvilinear segments [Fig. 1]. The straight-line fit, of course, is the old-fashioned method of constant gradients. Although the limitations of this approach are well known, it is still occasionally useful and has been retained as an option. The curvilinear segments are of the same form as those employed by Pedersen and Gordon [Ref. 3], in which the reciprocal of c^2 is quadratic in depth. The curve-fitting technique is completely automatic. It is basically similar to that of Gordon [Ref. 4], though it differs considerably in detail.

In addition to the profile layer depths, a set of special receiver depths may be read into the program, and a composite table of up to 100 depths and sound speeds is formed.

Each individual ray is specified by its source angle, from which the ray vertex velocity is computed. As a consequence of the assumption of horizontal stratification, the vertex velocity of each ray is constant, and the ray travels in a set of repetitive cycles between its upper and lower vertices. As a result, it is possible to pre-compute the increments of range, travel time, etc., in each layer. The tracing of the ray then consists simply of adding up the increments and computing the propagation loss as the ray proceeds outward in range.

The ray output data consist of the following: depth, range, ray angle, travel time, spreading loss, and propagation loss at up to six frequencies.

The actual tracing of rays is a relatively minor part of the NAVAIRDEVCEN ray-tracing program. The bulk of the program consists of four executive routines and their associated subroutines, which

contain the logic for determining what rays should be computed. The four executive routines are: (a) limiting rays, (b) ray families, (c) target rays (from source to specified receiver location, and (d) constant loss contours (used chiefly for multipath propagation loss versus range).

The first two routines are more or less straightforward items which, I suppose, are common to all ray-tracing programs. The limiting ray routine may be used to compute limiting rays to any desired local maximum of the velocity profile. It may also be used to compute families of rays in the vicinity of limiting rays. The only unusual feature of the ray family routine is the method of specifying the ray source angles. The data input format is extremely flexible, allowing any desired combination of individual rays and incremental sets of rays to be specified.

The target ray routine is designed to provide complete detailed information regarding multipath propagation between a specified source and a specified receiver location. It contains a search and iteration procedure which computes the source angle of each ray. After all the target rays have been computed, it then combines the rays in three different ways to obtain a resultant effective propagation loss:

(a) Strongest ray only.

(b) Intensities added (random phase).

(c) Amplitudes added (including phase interference computed from ray travel times).

The first is not really a combination, but merely gives the loss corresponding to the single strongest ray. The second method of combination consists of adding ray intensities, assuming random phase. The third method computes the relative phases, based on the ray travel times, and computes a loss based on pressure addition, phase included.

The constant loss contour routine has turned out in practice to be a misnomer since the contour portion of it is seldom used. This routine is a sort of "quick and dirty" target ray routine, designed to handle thousands of receiver locations instead of one. First of all, it computes a large family of rays and then interpolates between pairs of adjacent rays to determine the ray intensities at each of the specified receiver locations. It then adds the intensities of all the rays which reach each receiver location and computes the resultant propagation loss. The user has also the option of selecting the strongest ray only, but the pressure addition option is not available in this routine.

An optional second stage of this routine provides for a second interpolation to compute the ranges at each receiver depth at which the propagation loss is equal to a set of specified contour values, thus providing data for drawing contours of constant propagation loss.

We also have a modified version of the constant loss contour routine in which the printer prints a symbol at each point in a grid of 200 ranges and 40 depths. A different symbol is used for each 3 dB interval of propagation loss from 59 dB to 110 dB. After the array has been printed, it is a simple matter to draw contour lines manually.

TARGET RAYS

After this rather sketchy description of the program, I should like now to discuss the target ray procedure in somewhat more detail. The basic problem here is to find the source angles of the rays which propagate from a given source location to a given receiver location.

A simple graphical solution to the problem may be obtained by computing a large number of rays and plotting the ranges at the target

depth against the ray source angles. Consider the sample velocity profile shown in Fig. 2. Let the source be at the depth S within the deep sound channel, and let the target be at the depth T, slightly above the source. Before proceeding to the graph of range versus source angle, let us note some of the salient features of the propagation in this example. First, there will be a sector of rays, with source angles near the horizontal, which are trapped in the deep sound channel and do not reach the target depth. Secondly, as the source angle increases, both above and below the horizontal, there will be sectors of rays which penetrate above the target depth, but remain within the channel. These sectors are bounded by the limiting ray to the bottom of the surface duct. Thirdly, as the source angle increases further, there will be rays which reach the surface but are refracted before reaching the bottom. These rays represent RSR propagation. Finally, beyond the limiting ray to the bottom, and extending to $\pm 90^{\circ}$, there are the outermost sectors containing the rays which strike both the surface and the bottom.

If we now trace a large number of rays and plot the range at the target depth as a function of ray source angle, we get the rather strange-looking family of curves shown in Fig. 3. The different curves of the family correspond to successive crossings of the target depth as the rays move outward in range. Thus, each curve can be identified by the number of vertices through which the rays have passed. The innermost vertical dashed lines represent the rays tangent to the target depth. The central sector between these lines is a blank sector. It contains no rays which reach the target. Proceeding outward, the next pair of vertical lines, one on either side, correspond to the limiting rays to the bottom of the surface duct, while the outermost vertical lines correspond to the limiting rays to the bottom of the ocean. These limiting rays divide the angular region into sectors within which the various types of propagation occur — SOFAR channel, RSR, and bottom-surface bounce.

The graphical solution for a target at 50 kyd is indicated by the horizontal line drawn across the graph at that range. Each intersection of this line with one of the curves yields the source angle of a target ray.

The question now arises, how does one implement such a solution on a digital computer? Since an analytic solution is impossible, the most obvious approach is to use an iteration procedure, but there still remains the problem of making suitable initial estimates. This is where the concept of limiting rays and sectors is useful, since it is clearly not permissible to iterate across a sector boundary. Once the sectors have been defined, a search and iteration procedure is carried out separately in each sector.

Time will permit only a few brief comments about the procedures used in the program. First of all, we distinguish between the outer sector rays, i.e., those rays which bounce off both the surface and bottom, and the inner sector rays, i.e., those rays which experience refractive vertices, either upper or lower, or both.

As may be seen in Fig. 3, the range curves have no maxima or minima in the outer sectors. They are monotonic functions of the source angle. To see why, let us "unfold" the ocean, as indicated in Fig. 4. If we consider the extensions of two adjacent rays into the "unfolded" regions, as indicated by the dashed lines, we see that the rays continue to spread out and never cross one another. This behaviour permits an extremely simple search and iteration procedure. We start with a source angle slightly beyond the sector boundary and employ Newtonian iteration to find the first ray which reaches the target. We count the total number of vertices passed. To find the next ray, we use the preceding target ray as an initial estimate and iterate again, requiring this time that the ray pass through one more vertex. The process is continued in this manner until the desired number of outer sector rays have been found.

The problem of finding rays in the inner sectors is more complicated, and I must restrict the discussion to a brief statement of the basic concept. Each sector is divided into four equal intervals, and a separate search is conducted in each interval. The concept is illustrated in Fig. 5. Let θ_1 and θ_2 be the bounding source angles of the interval. As each of these rays is traced, the range is noted each time the ray crosses the target depth. Also, the number of ray vertices is counted. As soon as the target range has been exceeded, the number of vertices is recorded. Let the respective numbers be N_{V1} and N_{V2}. If N_{V1} and N_{V2} are the same, as indicated by the left-hand diagram, there is no target ray in the interval. If N_{V1} and N_{V2} differ by 1, as indicated in the centre diagram, there is one ray, and it is found by an iteration procedure based on interpolation. If N_{V1} and N_{V2} differ by more than 1, the interval is divided by 2 and the process is repeated.

The target ray routine in our ray-tracing program has proved very successful and has been used extensively in studying multipath propagation. Because of the accuracy with which travel times can be computed, it is particularly useful for investigating the effects of phase interference.

COMPARISON WITH NORMAL MODE THEORY

In presenting a few results obtained with our ray-tracing program, I shall concentrate on the phenomenon of phase interference. Consider first of all a comparison with normal mode theory. We have developed a number of normal mode programs, one of which is based on a three-layer model in which $1/c^2$ varies linearly with depth in each layer. With a three-layer model it is possible to approximate a typical deep-ocean velocity profile containing a surface duct. The upper graph of Fig. 6 is a plot of propagation loss versus range for a three-layer profile without a surface duct, i.e.,

the surface layer has a negative gradient. At the bottom of Fig. 6 is a comparison run made with the ray-tracing program, using the same bottom parameters and approximately the same velocity profile.

Except for the convergence zone, the agreement between the two curves is quite remarkable, even down to the short-period oscillations. The most puzzling feature, however, is the convergence zone. Although it is to be expected that the detailed structure of the zone as predicted by ray theory should be inaccurate, it is quite surprising to find that the entire outer portion of the ray theory zone is missing from the normal mode curve. Investigation of this problem has revealed that the entire outer portion of the zone predicted by ray theory is formed by a small bundle of rays leaving the source within $\pm 2^\circ$ of the horizontal. According to ray theory, the energy radiated into this small bundle should stay intact as the rays propagate and should become concentrated in a small region at the convergence zone. Apparently, however, diffraction effects are sufficiently important to cause the energy to spread out beyond the geometric confines of the ray bundle and to become widely diffused before it reaches the range of the convergence zone. It appears that one must be very cautious about using simple ray theory to make predictions of this sort.

The dashed curve in the lower figure shows the propagation loss computed on the basis of random-phase intensity addition.

COMPARISON WITH EXPERIMENT

It is commonly assumed that phase coherence is lost in bottom-bounce propagation in the deep ocean. However, this is not necessarily the case. The large fluctuations which are observed in propagation loss are evidence of phase interference effects, and in some instances these fluctuations show some correlation with ray-theory predictions. Figure 7 shows some results of an experiment conducted near the Bahamas a few years ago. Ten sonobuoys were dropped at various points

along a straight line, and a source ship, towing a CW projector, proceeded along the line. Values of propagation loss computed from the various hydrophone outputs were superimposed on the same range scale, resulting in the various "wiggly" segments shown in the figure. At any given range on the graph, the curves thus correspond to different ship locations for the different buoys. In spite of the spread of the results, it can be seen that certain distinct trends stand out. In particular, a large scallop may be seen, extending from 20 kyd to about 40 kyd. Beyond this is another broad scallop extending out to the convergence zone.

The heavy line on the graph shows the propagation loss predicted by the ray-tracing program, assuming phase coherence. Although there are slight discrepancies in the predicted ranges, the main features of the theoretical curve at ranges beyond 20 kyd are in sufficient agreement with the experimental data as to leave little doubt as to the existence of phase-coherent propagation. At ranges shorter than 20 kyd the scatter of the experimental data is too large to exhibit a consistent pattern. Also, at ranges beyond the first convergence zone the correlation between the experimental and theoretical propagation loss is poor, suggesting that phase coherence is lost after the second bounce.

A SUGGESTED RAY COMPUTATION PROCEDURE FOR GENERAL SOUND SPEED VERSUS DEPTH RELATION

The use of curvilinear segments permits the construction of a velocity profile curve in which the slope is everywhere continuous. This is obviously a great improvement over the use of straight line segments, where the discontinuities in slope at the layer boundaries give rise to false caustics and shadow zones. However, with the quadratic functions currently used in the ray-tracing program, it is impossible to avoid discontinuities in the second derivative at the points where adjacent segments are joined. Discontinuities in the second derivative, while not as serious as discontinuities in slope, are nevertheless capable of causing undesirable kinks in the curve of propagation loss versus range.

To treat the more general case in which functional forms are used which permit continuity of both first and second derivatives, consideration has been given to the use of numerical integration. The integrals involved in the computation of horizontal range, travel time, and spreading loss are:

Horizontal range

$$x = \sum \Delta x \qquad \Delta x = \int_{z_1}^{z_2} \frac{\cos\theta}{\sin\theta}\, dz$$

Travel time

$$t = \sum \Delta t \qquad \Delta t = \frac{1}{C_V} \int_{z_1}^{z_2} \frac{1}{\sin\theta \cos\theta}\, dz$$

Spreading loss

$$N_{spr} = 10 \lg \left| \frac{xu \sin\theta_o \sin\theta}{r_1^2 \cos^2\theta_o} \right|$$

$$u = \sum \Delta u \qquad \Delta u = \int_{z_1}^{z_2} \frac{\cos\theta}{\sin^3\theta}\, dz$$

where

z	=	depth
θ	=	$\theta(z)$ ray angle
θ_o	=	ray angle at source
C	=	$C(z)$ = sound speed
C_o	=	sound speed at source
C_V	=	$C_o/\cos\theta_o$ = vertex velocity
$\cos\theta$	=	C/C_V
r_1	=	1 yd

The spreading loss is usually expressed in terms of the range derivative $\partial x/\partial\theta_o$. If instead of this derivative, we use a related parameter u, as indicated above, the integrals for the increments Δx, Δt, and Δu in each layer all have a similar form.

In general, numerical integration appears to be an attractive method of evaluating these integrals. There is a problem, however, at a refractive vertex, where the ray becomes horizontal and hence the ray angle θ is zero. At such a point the integrands of both Δx and Δt blow up (although the integrals are finite), and the Δu integral itself blows up.

Let us now transform the integrals by expressing $1/C^2$ as a function $P(z)$, which might logically, though not necessarily, be chosen to be a polynomial in z. With this transformation, the integrals appear as follows. Let

$$P(z) = 1/C^2$$
$$P_V = 1/C_V^2$$
$$Q = P - P_V$$

then

$$\Delta x = \sqrt{P_V} \int_{z_1}^{z_2} \frac{dz}{\sqrt{Q}}$$

$$C_V \Delta t = \sqrt{P_V}\ \Delta x + \int_{z_1}^{z_2} \sqrt{Q}\ dz$$

$$\Delta u = \Delta x + P_V^{3/2} \int_{z_1}^{z_2} \frac{dz}{Q^{3/2}} \quad .$$

Note: At a refractive vertex,

$$C = C_V$$
$$P = P_V$$
$$Q = 0$$

The limits of integration z_1 and z_2 are the depths of the upper and lower boundaries of the layer. The travel time Δt is now well behaved, but problems still remain in Δx and Δu, since the function Q goes to zero at a refractive vertex.

The problem can be circumvented by removing Q from the denominator through integration by parts, once for Δx and twice for Δu. Let

$$P' = \frac{dP}{dz} = \frac{dQ}{dz} \quad \text{so that} \quad dz = \frac{dQ}{P'}$$

$$\Delta x = \sqrt{P_V} \int_{z_1}^{z_2} \frac{dQ}{P'\sqrt{Q}}$$

$$= 2\sqrt{P_V} \left[-\frac{\sqrt{Q}}{P'} \Bigg|_{z_1}^{z_2} + \int_{z_1}^{z_2} \frac{P''\sqrt{Q}}{P'^2} \right]$$

$$\Delta u = \Delta x + P_V^{3/2} \int_{z_1}^{z_2} \frac{dQ}{P'Q^{3/2}}$$

$$= \Delta x - 2P_V^{3/2} \left[\left(\frac{1}{P'\sqrt{Q}} + \frac{2P''\sqrt{Q}}{P'^3} \right) \Bigg|_{z_3}^{z_2} + 2 \int_{z_1}^{z_2} \left(\frac{3P''^2}{P'^4} - \frac{P'''}{P'^3} \right) \sqrt{Q}\, dz \right]$$

(Note: when $Q = 0$ omit term $\frac{1}{P'\sqrt{Q}}$).

Except for the term $1/P'\sqrt{Q}$ in the formula for Δu, the only function appearing in the denominators is the derivative P'. This function is zero only at a local extremum (i.e., maximum or minimum) of the velocity profile. Hence these formulae can be used for any profile segment which does not contain an extremum. In the special case where a vertex occurs within a segment containing an extremum, it is a simple matter to divide the segment into two parts, using the basic formulae in one part and the transformed formulae in the other.

A final comment is in order regarding the term $1/P'\sqrt{Q}$, which becomes infinite at the vertex. This is a problem which is common

to all spreading loss computations based on the range derivative. The value of u is infinite at a refractive vertex, and the spreading loss there must be computed by a special formula which does not involve u. However, values of u are required at points beyond the vertex. It will be noted that in passing through the vertex, the infinite term occurs twice — once in the interval immediately preceding the vertex, and again in the interval immediately following. It can be shown that the correct answer is obtained simply by ignoring this term altogether.

A small computer program was written to check out this approach. Two simplified types of curve-fitting were included, one based on segments in which $P(z)$ is quadratic in z, as in the NAVAIRDEVCEN ray-tracing program, and the other based on a spline fit of segments in which $P(z)$ is a cubic. Figure 8 shows a sample velocity profile consisting of four quadratic segments. At the right of the figure is an expanded-scale plot of the difference between the quadratic fit and the spline fit. Except for the first 100 ft at the top, which will not concern us, the profiles differ by less than 0.2 ft/s.

A source was placed near the bottom at a depth of 1170 ft, and a family of rays were traced up over the first vertex and down again until they reached the source depth. The effects of the discontinuities in the second derivative may be expected to show up in those rays which vertex in the vicinity of the layer boundaries A, B and C.

In Fig. 9 the spreading loss is plotted as a function of ray source angle for both the quadratic fit and the spline fit. The source angle scale has been chosen to show the effects of the two layer boundaries A and B. (The effect of boundary C would be off-scale at the right.) The effects of the discontinuities are indicated by the kinks in the solid curve at the points A and B. The spike immediately beyond A represents a focal point resulting from the nature of the velocity profile.

The spline fit is represented by the dashed curve, which does not exhibit the discontinuities in slope. The oscillatory nature of this curve to the left of the focal point is a result of the rather simple-minded technique of forcing the spline curve to pass rigorously through all the data points. With a little more care, it would be possible to obtain better results.

Figure 10 shows another sample velocity profile consisting of three layers and exhibiting a reverse curvature. The difference between the spline and quadratic fits is shown at the right. The accompanying plot of spreading loss versus source angle is shown in Fig. 11, where, as before, kinks occur in the quadratic-fit curve in the vicinity of the layer boundaries A and B.

In making these runs, it has been found that the special formulae based on integration by parts should be used not only in intervals where a refractive vertex actually occurs, but also where a vertex is merely approached, that is, where the ray angle approaches within a degree or so of the horizontal. The transformed integrals have proven to be exceedingly well behaved in all examples investigated.

It is doubtful whether the errors arising from discontinuities in the second derivative of the profile curve are serious enough to warrant the inclusion of this approach into general ray-tracing programs. However, if special situations arise in which continuity of the second derivative is important, the technique suggested above appears to be quite appropriate. Furthermore, because virtually no restrictions are placed on the mathematical form of the fitting function, it should be possible to fit most velocity profiles with a relatively small number of segments.

REFERENCES

1. C.L. Bartberger and T.L. Stover, "The NADC Ray-Tracing Program", Report No. NADC-SD-6833, 4 November 1968.

2. W.D. Wilson, "Equation for the Speed of Sound in Sea Water", J. Acoust. Soc. Am., Vol. 32, p. 1357, October 1960.

3. M.A. Pedersen, D.F. Gordon and Alice Joy Keith, "A New Ray Intensity Procedure for Underwater Sound Based on a Profile Consisting of Curvilinear Segments (U)", Navy Electronics Laboratory (Naval Undersea Research and Development Center) Report No. 1105, 30 March 1962, CONFIDENTIAL.

4. D.F. Gordon, "Extensions of the Ray Intensity Procedure for Underwater Sound Based on a Profile Consisting of Curvilinear Segments (U)", Navy Electronics Laboratory (Naval Undersea Research and Development Center) Report No. 1217, 3 April 1964, CONFIDENTIAL.

DISCUSSION

In reply to queries, Bartberger confirmed that only one ray was used for intensity calculations.

When comparing results between ray theory and normal mode calculations, a profile with C^{-2} linear in depth was assumed for the latter. This was approximated for the ray tracing by closely spaced segments in which C^{-2} was quadratic in depth.

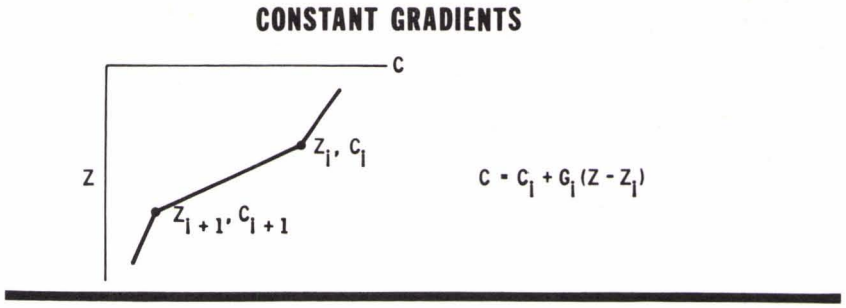

FIG. 1

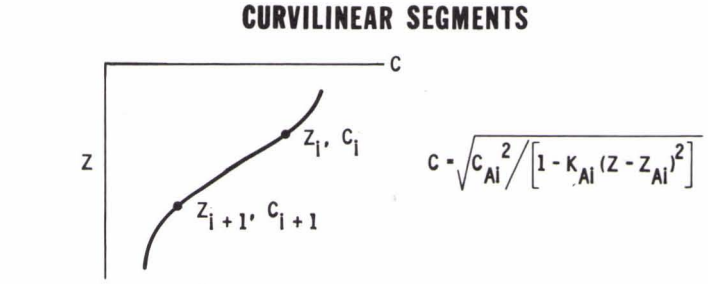

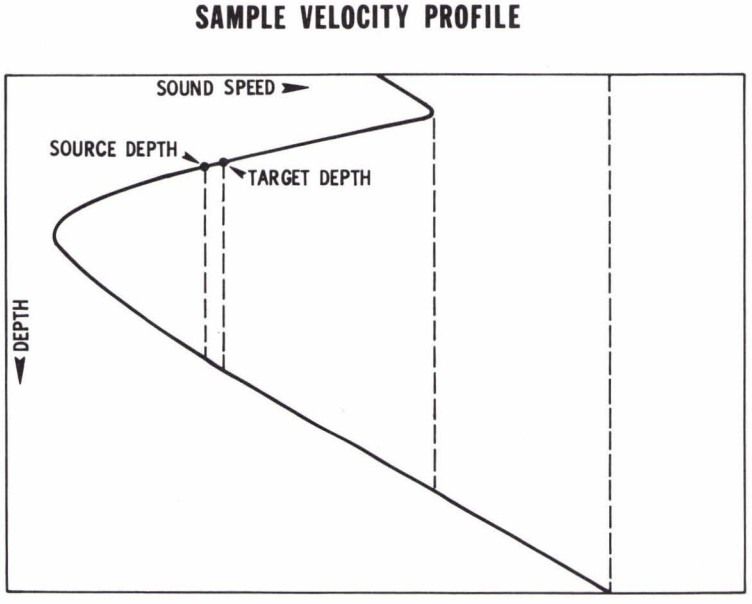

FIG. 2

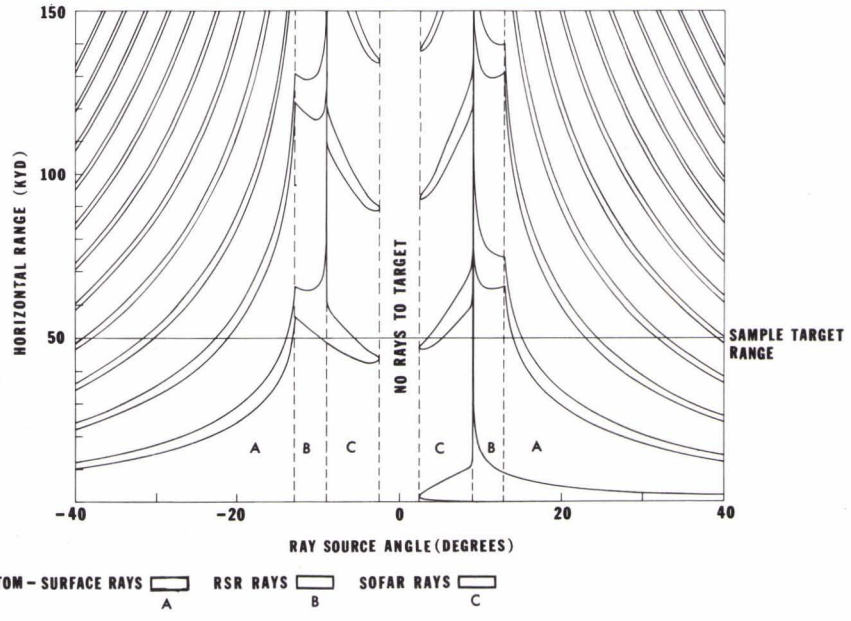

FIG. 3

BEHAVIOR OF OUTER SECTOR RAYS

(WHEN "UNFOLDED," THEY NEVER CROSS EACH OTHER)

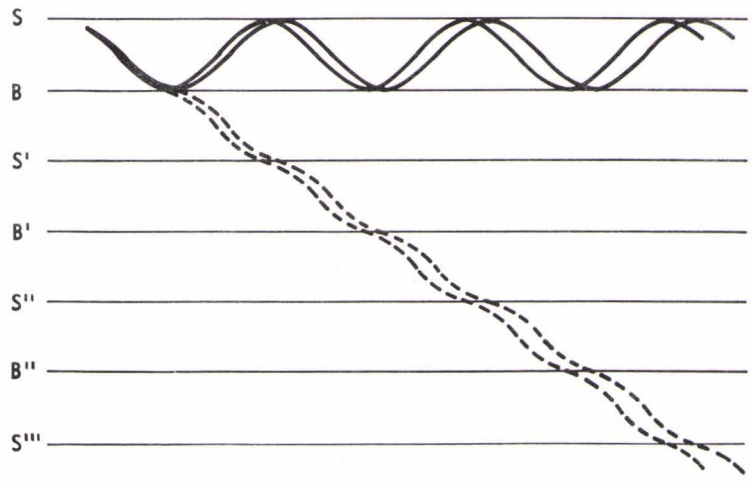

FIG. 4

INNER SECTOR TEST FOR TARGET RAYS

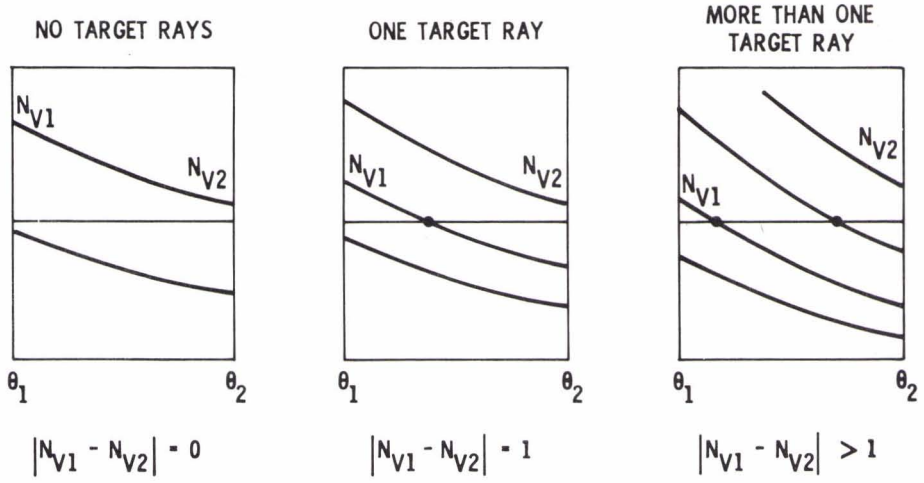

FIG. 5

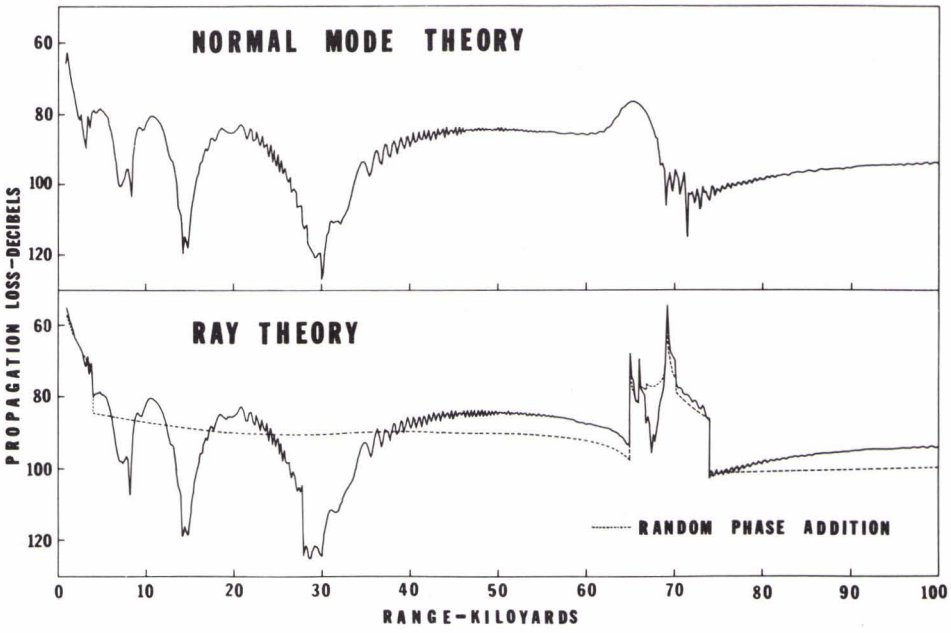

FIG. 6

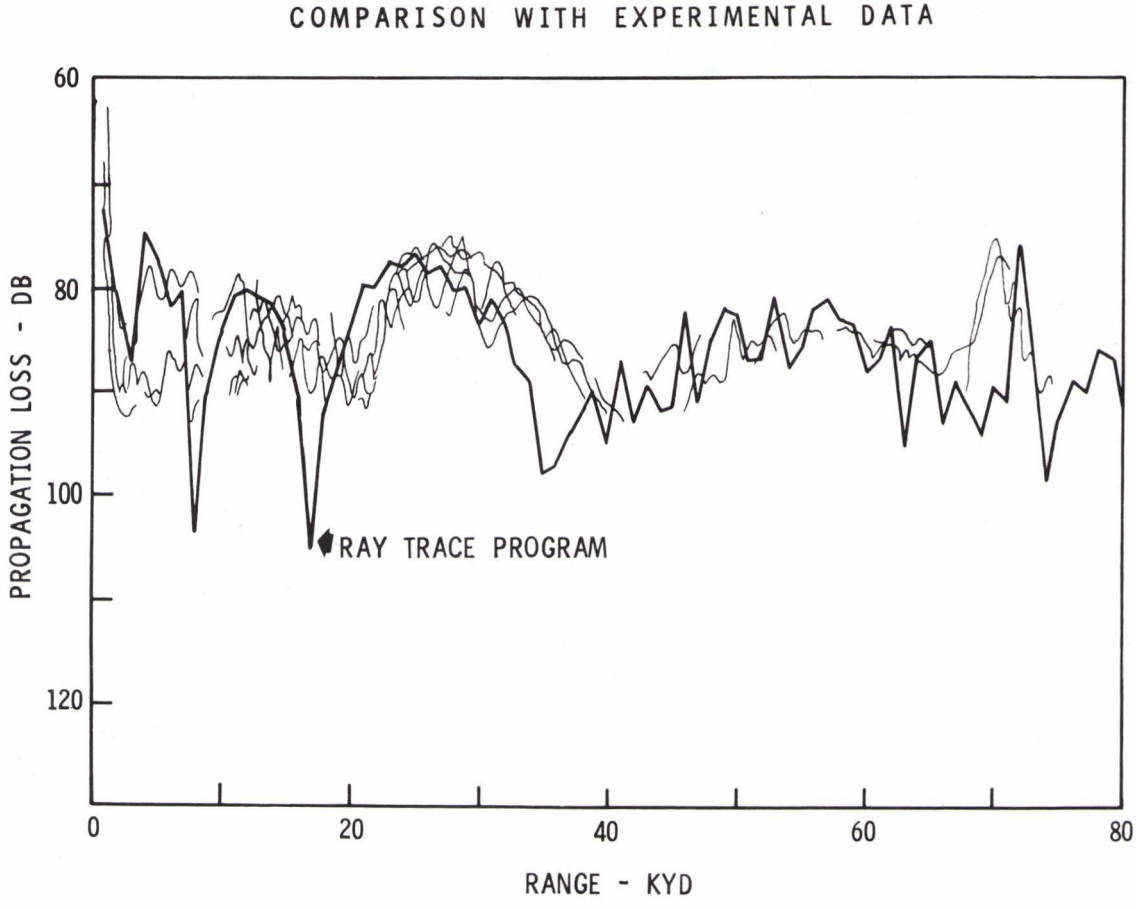
COMPARISON WITH EXPERIMENTAL DATA
PROPAGATION LOSS - DB
60
80
100
120
RAY TRACE PROGRAM
0
20
40
60
80
RANGE - KYD

FIG. 7

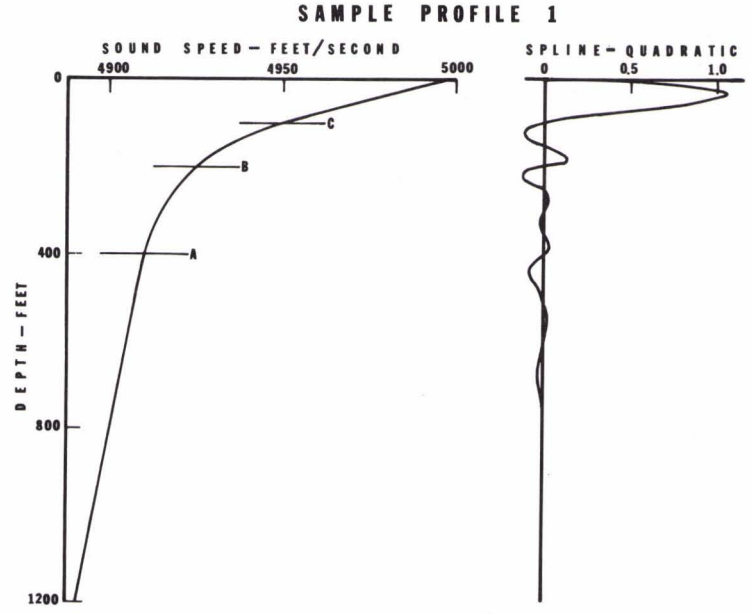
SAMPLE PROFILE 1
SOUND SPEED - FEET/SECOND
4900
4950
5000
SPLINE - QUADRATIC
0
0.5
1.0
0
400
800
1200
DEPTH - FEET
A
B
C

FIG. 8

SAMPLE PROFILE 1

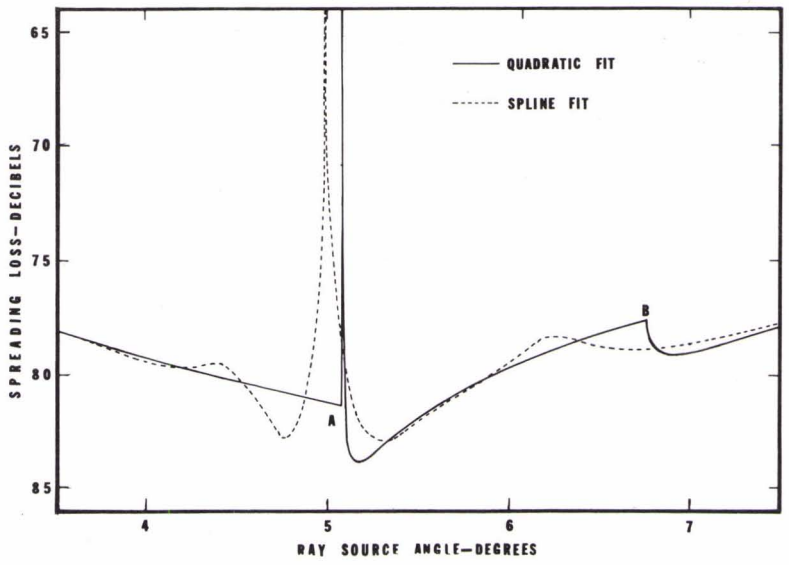

FIG. 9

SAMPLE PROFILE 2

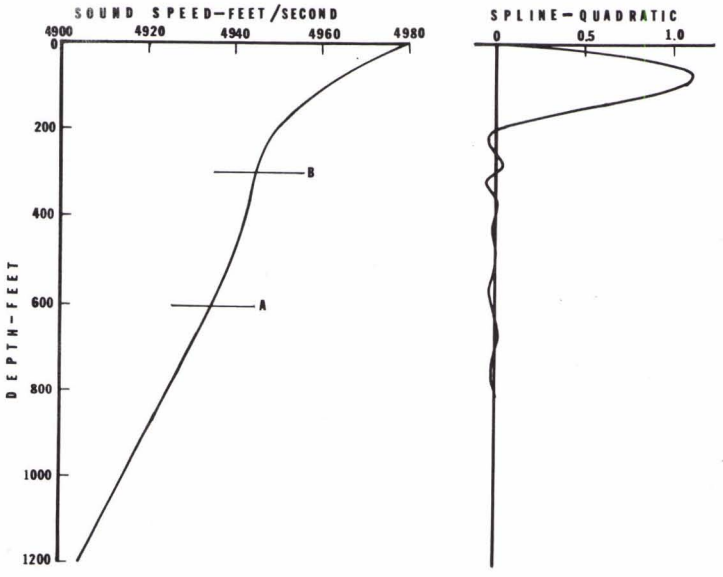

FIG. 11

SAMPLE PROFILE 2

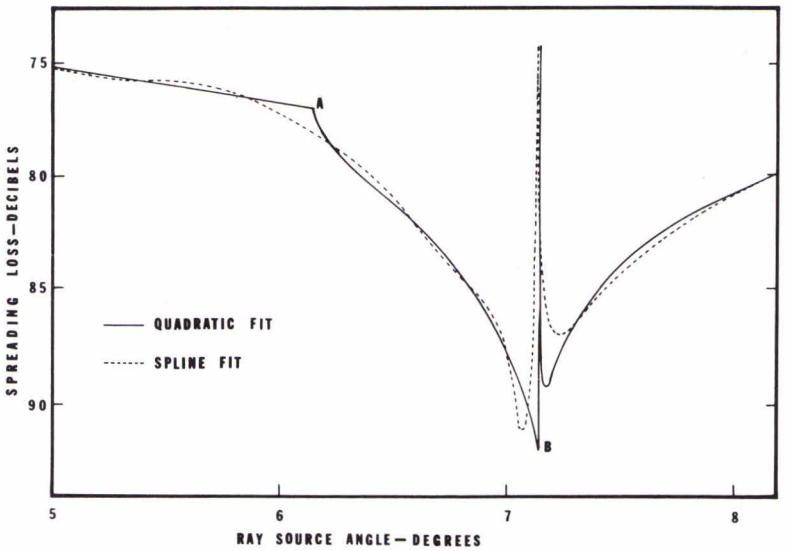

FIG. 10